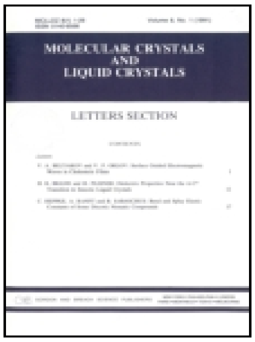

Taylor & Francis
Taylor & Francis Group

Molecular Crystals and Liquid Crystals

ISSN: 1542-1406 (Print) 1563-5287 (Online) Journal homepage: http://www.tandfonline.com/loi/gmcl20

Luminescence of Terbium (III) Complexes Incorporated in Carboxylic Acid Functionalized Polystyrene/BaTiO$_3$ Nanocomposites

Xuan Thang Cao, Ali Md Showkat, Won-Ki Lee & Kwon Taek Lim

To cite this article: Xuan Thang Cao, Ali Md Showkat, Won-Ki Lee & Kwon Taek Lim (2015) Luminescence of Terbium (III) Complexes Incorporated in Carboxylic Acid Functionalized Polystyrene/BaTiO$_3$ Nanocomposites, Molecular Crystals and Liquid Crystals, 622:1, 36-43, DOI: 10.1080/15421406.2015.1096988

To link to this article: http://dx.doi.org/10.1080/15421406.2015.1096988

Mol. Cryst. Liq. Cryst., Vol. 622: pp. 36–43, 2015
Copyright © Taylor & Francis Group, LLC
ISSN: 1542-1406 print/1563-5287 online
DOI: 10.1080/15421406.2015.1096988

Luminescence of Terbium (III) Complexes Incorporated in Carboxylic Acid Functionalized Polystyrene/BaTiO$_3$ Nanocomposites

XUAN THANG CAO,[1] ALI MD SHOWKAT,[1] WON-KI LEE,[2]
AND KWON TAEK LIM[1,*]

[1]Department of Imaging System Engineering, Pukyong National University, Busan, Korea
[2]Department of Polymer Engineering, Pukyong National University, Busan, Korea

Luminescence nanocomposites based on barium titanate nanoparticles (BaTiO$_3$), polystyrene (PSt), and terbium ion (Tb^{3+}) were synthesized by using a combination of reversible addition fragmentation chain transfer polymerization, Friedel-Crafts alkylation reaction and coordination chemistry. The modification of the surface of BaTiO$_3$ was conducted by an exchange process with S-benzyl S'-trimethoxysilylpropyltrithiocarbonate to anchor macro-initiators for the polymerization of styrene. Subsequently, PSt grafted barium titanate was functionalized by the substitution reaction between 4-(chloromethyl) benzoic acid and PSt to produce hybrids, BaTiO$_3$-g-PSt -COOH. The coordination of the hybrids with Tb^{3+} ions in the presence of 1,10-phenanthroline (Phen) afforded fluorescent Tb^{3+} tagged carboxylic acid functionalized polystyrene/barium titanate (BaTiO$_3$-g-PSt-Tb^{3+}-Phen). FT-IR, XRD, TGA, and SEM analyses revealed the formation of BaTiO$_3$-g-PSt-Tb^{3+}-Phen hybrids. The optical properties of BaTiO-$_3$-g-PSt-Tb^{3+}-Phen were investigated by using fluorescence spectroscopy.

Keywords Luminescence; RAFT polymerization; Friedel-Crafts alkylation reaction; rare earth element

Introduction

Nanomaterials have been widely applied in a variety of fields such as electronics, optics, energy, catalyst, biology, and medicine in the past decade [1, 2]. Recently, barium titantate (BaTiO$_3$) has captured special attention among these materials, as more information has been disclosed by studies on the photoluminescence (PL) in BaTiO$_3$ [3]. BaTiO$_3$ is able to emit the PL phenomenon at room temperature in the form of amorphous powder as well as nanocrystals, and PL could result from the effect of either quantum confinement or defect [4]. Zhang *et al.* reported that the PL property of BaTiO$_3$ is related to short Ti–O atomic distances into the regular octahedral of the BaTiO$_3$ unit cell and the charge transfer

---

[*] Address correspondence to Kwon Taek Lim, Department of Imaging System Engineering, Pukyong National University, 599-1 Daeyeon-3-Dong, Nam gu, Busan 608-737, Korea. E-mail: ktlim@pknu.ac.kr

Color versions of one or more of the figures in the article can be found online at www.tandfonline.com/gmcl.

between titanium and oxygen atoms [5]. Verma *et al.* showed PL in pure BaTiO$_3$ and Fe doped BaTiO$_3$ nanostructures [6]. Currently, lanthanide (Ln) doped inorganic or organic materials have attracted much interest due to their potential applications as luminescence probes, sensors in chemical or biological systems [7]. Most studies on Ln elements are europium (Eu) and terbium (Tb) whose PL properties have stimulated great interest in developing photoactive materials for biological applications [8, 9].

Taking the above consideration into account, we have devised a protocol to synthesize terbium doped hybrids of polystyrene grafted barium titanate (BaTiO$_3$-*g*-PSt-Tb^{3+}) based on the combination of reversible addition fragmentation chain transfer (RAFT) polymerization, Friedel-Crafts substitution reaction, and coordination chemistry. Polystyrene grafted BaTiO$_3$ bearing multi-carboxyl groups on the external layers were coordinated with triplet Tb^{3+} ions in the presence of 1,10-phenanthroline (Phen) to afford BaTiO$_3$-*g*-PSt-Tb^{3+}-Phen complexes (Scheme 1).

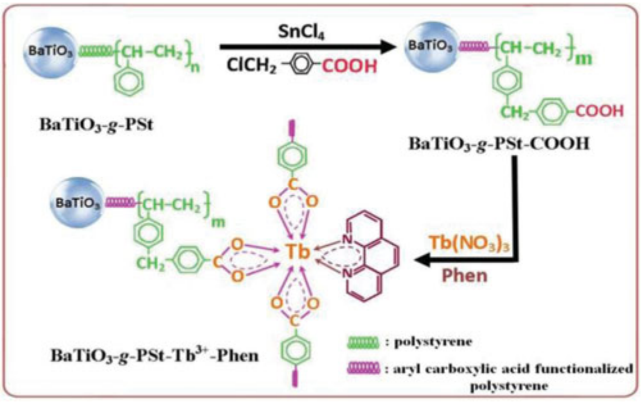

Scheme 1. Synthesis of BaTiO$_3$-*g*-PSt-Tb^{3+} hybrids in the presence of Phen.

Experimental Details

Materials

All chemicals were purchased from Sigma-Aldrich (Korea). Styrene was distilled under vacuum prior to use. 2,2′-Azobis(isobutyronitrile) (AIBN) (98%) was recrystallized in methanol before use. 4-(Chloromethyl) benzoic acid (CMBA, 95%), 1,10-phenanthroline (Phen, $\geq$99%), Tb(NO$_3$)$_3$.6H$_2$O (99.99%), tin(IV) chloride (SnCl$_4$, 99.99%), (3-mercaptopropyl) trimethoxysilane (95%), carbon disulfide (CS$_2$, $\geq$99%), benzyl bromide (98%), and solvents of analytical grade were used as received. BaTiO$_3$ (<100 nm, $\geq$99%) was supplied by the Display and Lighting Phosphor Bank at Pukyong National University.

Synthesis of S-benzyl S′-trimethoxysilylpropyltrithiocarbonate (RAFT Agent)

Briefly, a solution of (3-mercaptopropyl)trimethoxysilane (95%, 6.20 g) in 50 mL of anhydrous methanol was added dropwise to a solution of sodium methoxide in methanol (25 wt%) under nitrogen. After stirring for 30 min, CS$_2$ (3.05 g) was added dropwise to the solution and stirred for 5 h. To the yellow solution was added benzyl bromide (98%, 5.24 g), and the mixture was stirred overnight under nitrogen. The RAFT agent was concentrated, diluted with dichloromethane, filtered off, and concentrated under reduced pressure [10]. ^{1}H NMR ($CDCl_3$): 7.30 (m, 5H, PhH), 4.60 (s, 2H, CH_2), 3.56 (s, 9H, CH_3O), 3.39 (t, 2H, CH_2S), 1.84 (m, 2H, CH_2), 0.77 (t, 2H, CH_2Si).

Immobilization of RAFT Agent onto $BaTiO_3$ Nanoparticles ($BaTiO_3$-RAFT)

In a typical procedure, $BaTiO_3$ (2.0 g) and toluene (60 mL) were put in a three-neck flask under nitrogen. The deoxygenated RAFT agent (2.0 g) in 15 mL of toluene was added into the mixture by a syringe. The reaction mixture was refluxed overnight and then maintained at 120°C for another 3 h. The product was filtered, washed, and extracted with dichloromethane and dried under vacuum for 24 h.

Synthesis of $BaTiO_3$-g-PSt-COOH Composites

Polystyrene grafted barium titanate ($BaTiO_3$-*g*-PSt) were prepared as follows: $BaTiO_3$-RAFT (0.2 g), styrene (2.0 g), AIBN (0.2 g), and DMF (2.0 mL) were placed in a round-bottom flask and kept stirring for 12 h at 80°C under nitrogen. The product was purified by precipitating in an excess amount of methanol, filtering, washing with DMF, and drying under vacuum at 40°C for 48 h. In the procedure for cleavage of the grafted polymers, 100 mg of $BaTiO_3$-*g*-PSt was added into the mixture of 5 mL of THF and one drop of a dilute aqueous solution of $Na_2S_2O_4$. The solution was degassed with nitrogen and then 0.1 mL of n-hexylamine was injected into the mixture. After stirring overnight, the solution was filtered off, and the recovered PSt was subjected to GPC analysis (M_n = 11200, PDI = 1.54). $BaTiO_3$-*g*-PSt-COOH were synthesized as follows: $BaTiO_3$-*g*-PSt (0.5 g), CMBA (0.2 g), $SnCl_4$ (0.026 g), and N,N-dimethylacetamide (5.0 mL) were put into a round-bottom flask and refluxed at 70°C for 15 h. The mixture was precipitated in methanol, filtered, and washed with dilute HCl to remove $SnCl_4$. The product was washed with ethanol and deionized water repeatedly, and dried under vacuum at 40°C for 24 h.

Synthesis of $BaTiO_3$-g-PSt-Tb^{3+}-Phen Hybrids

A typical procedure for the synthesis of $BaTiO_3$-*g*-PSt-Tb^{3+}-Phen was as follows: 10 mL of a Phen (0.84 mmol) solution was added dropwise into the dispersion of $BaTiO_3$-*g*-PSt-COOH (0.30 g, 0.42 mmol of benzoic acid) in anhydrous DMF (15 mL) and the pH of solution was adjusted to 6–7. $Tb(NO_3)_3$ (0.42 mmol) dissolved in ethanol (5 mL) was dropped slowly into the solution. The mixture was stirred at 50°C for 8 h, followed by aging overnight. The product was precipitated into methanol, filtered, and washed with deionized water, and dried under vacuum at 40°C. Both complexes were prepared by using the same molar ratio in the same solvent in order to compare fluorescence properties of $BaTiO_3$-*g*-PSt-Tb^{3+} and Tb^{3+}-Phen.

Instrumentation

The nature of chemical bonds was studied by Fourier transformed infrared spectrophotometry (FT-IR) with a BOMEM Hartman & Braun FT-IR Spectrometer in the frequency range of 4000–400 cm^{-1}. The thermogravimetric analysis (TGA) was conducted with a Perkin-Elmer Pyris 1 analyzer (USA). TGA profiles were collected within the temperature

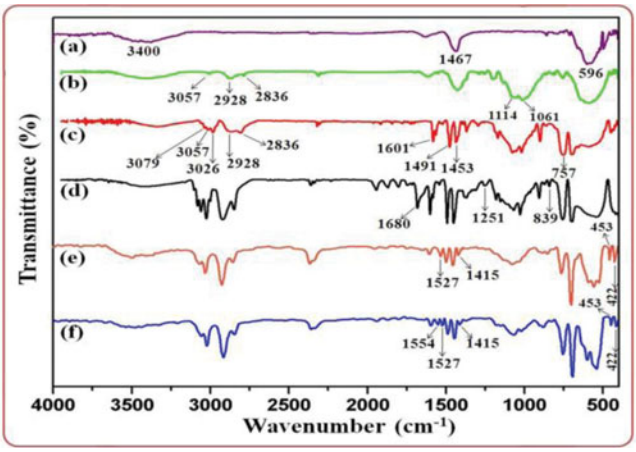

Figure 1. FT-IR spectra of (a) BaTiO$_3$, (b) BaTiO$_3$-RAFT, (c) BaTiO$_3$-*g*-PSt, (d) BaTiO$_3$-*g*-PSt-COOH, (e) BaTiO$_3$-*g*-PSt-Tb^{3+}, and (f) BaTiO$_3$-*g*-PSt-Tb^{3+}-Phen.

range of 50–800°C at a heating rate of 10°C min^{-1} under continuous nitrogen flow. The crystallographic state of the nanocomposites was studied by a Philips X'pert-MPD system diffractometer. The morphologies of the samples were investigated by a scanning electron microscope (SEM) equipped with energy dispersive X-ray spectrometer EDS (Hitachi JEOL-JSM-5 6700F system, Japan). Photoluminescence (PL) spectra were recorded on a F-4500 spectro-fluorometer (Hitachi, Japan) excited at 328 nm.

Results and Discussion

Figure 1 depicts the FT-IR spectra of the composites. The spectrum of BaTiO$_3$ (Fig. 1a) shows a broad band at 3400 cm^{-1} due to the -OH stretching vibration. The absorption bands at 1467 and 596 cm^{-1} are assigned to the stretching vibration of $CO_3{}^{2-}$ from the residual BaCO$_3$ and the vibration mode of a metal-dioxo bridge [11]. The chemical bond of the RAFT agent on the surface of BaTiO$_3$ showed the characteristic peaks at 2836 and 2928 cm^{-1} owing to methylene groups of the RAFT agent, and a weak but visible band at 3057 cm^{-1} assigning for the sp^2 C-H stretching of aromatic rings (Fig. 1b). The presence of absorption peaks at 1114 cm^{-1} (Si-O-particle) and 1061 cm^{-1} (Si-O-Si group) suggested that the silane was anchored onto BaTiO$_3$. The spectrum of BaTiO$_3$-*g*-PSt presented bands at 2836–3079 cm^{-1} and 1453 - 1601 cm^{-1} which were ascribed to the stretching vibration of C—H and C═C in the PSt chains (Fig. 1c). As expected, BaTiO$_3$-*g*-PSt-COOH exhibits new absorption bands at 1680 and 1251 cm^{-1} which are attributed to the C═O stretching vibration of carbonyl groups and the C—H plane bending vibration of 1,4-disubstituted benzene rings (Fig. 1d). The formation of BaTiO$_3$-*g*-PSt-Tb^{3+} was illustrated by the spectrum in Fig. 1e. It is clearly seen that the new bands at 1527 and 1415 cm^{-1} are implied to the asymmetric and symmetric vibration of the carboxylic group. In addition, the stretching vibration of a free carbonyl group at 1680 cm^{-1} disappeared and the stretching absorption of Tb-O bonds was observed at 422 and 453 cm^{-1}. This result demonstrated that the coordination between BaTiO$_3$-*g*-PSt-COOH and Tb^{3+} took place. The spectrum of BaTiO$_3$-*g*-PSt-Tb^{3+}-Phen is similar to the original BaTiO$_3$-*g*-PSt-Tb^{3+},

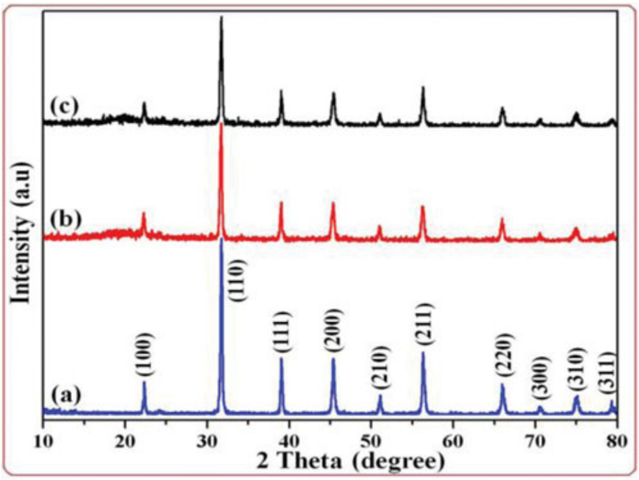

Figure 2. X-ray diffraction patterns of (a) $BaTiO_3$, (b) $BaTiO_3$-*g*-PSt, and (c) $BaTiO_3$-*g*-PSt-COOH.

as shown in Fig. 1f. However, a new peak at 1554 cm^{-1} indicates the additional stretching vibration of the C=N bond of Phen.

Figure 2 shows the XRD patterns of $BaTiO_3$, $BaTiO_3$-*g*-PSt, and $BaTiO_3$-*g*-PSt-COOH composites. It can be clearly seen that the peaks of $BaTiO_3$-*g*-PSt (Fig. 2b) and $BaTiO_3$-*g*-PSt-COOH (Fig. 2c) are perfectly indexed to the tetragonal phase of $BaTiO_3$ with 2θ values of 22.33°, 31.73°, 39.03°, 45.35°, 51.07°, 56.31°, 65.97°, 70.57°, 75.17°, and 79.33° corresponding to the crystal planes of (100), (110), (111), (200), (210), (211), (220), (300), (310), and (311), respectively (Fig. 2a). The XRD result revealed the grafting of the polymer did not alter the crystallinity of the $BaTiO_3$ nanoparticles.

TGA analyses were performed for thermal degradation, as shown in Fig. 3. $BaTiO_3$ lost 1.4% of weight due to the release of absorbed water. The weight loss of $BaTiO_3$-RAFT is 19% between 50 to 800°C because the encapsulating organic molecules decamped at

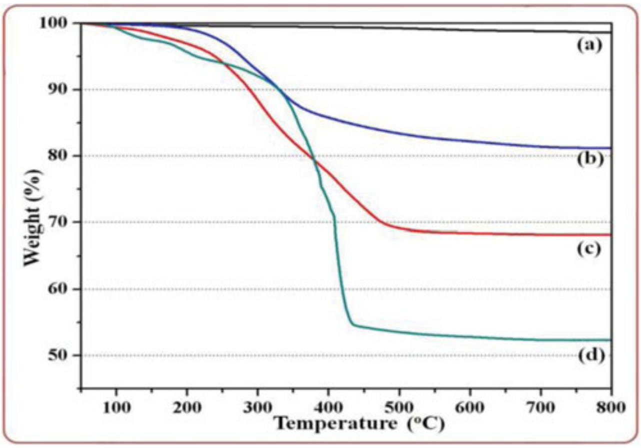

Figure 3. TGA spectra of (a) $BaTiO_3$, (b) $BaTiO_3$-RAFT, (c) $BaTiO_3$-*g*-PSt, and (d) $BaTiO_3$-*g*-PSt-COOH.

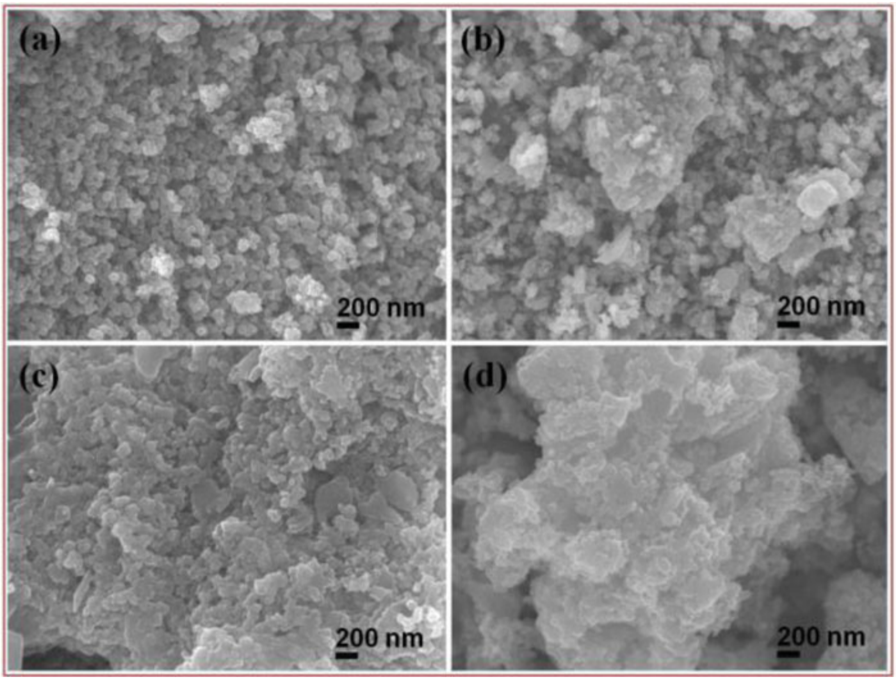

Figure 4. SEM pictures of (a) $BaTiO_3$, (b) $BaTiO_3$-RAFT, (c) $BaTiO_3$-*g*-PSt, and (d) $BaTiO_3$-*g*-PSt-COOH.

high temperature. $BaTiO_3$-*g*-PSt started to decompose at 230°C, and weight loss was 31% at 500°C due to the thermal degradation of grafted PSt. The as-prepared $BaTiO_3$-*g*-PSt-COOH were significantly degraded between 325 and 430°C and lost 48% at 800°C. Based on the TGA results, the content of carboxylic acid functionalized PSt can be calculated to be 24% indicating that the amount of the brush polymer is not too high and PSt-COOH were successfully decorated onto $BaTiO_3$.

The surface morphologies of $BaTiO_3$ and the composites can be visualized by using SEM characterization. The $BaTiO_3$-RAFT surface was turned in little extent in comparison to $BaTiO_3$, indicating the immobilization of the RAFT agent (Fig. 4b). After RAFT polymerization, the $BaTiO_3$-*g*-PSt image demonstrates relatively spherical shape having the polymer layer (Fig. 4c). Furthermore, $BaTiO_3$-*g*-PSt-COOH show the morphology with many spheres which nestle more closely due to the coverage of aryl carboxylic acid grafted polymer chains (Fig. 4d).

Figure 5 showed the emission spectra of $BaTiO_3$-*g*-PSt-Tb^{3+}-Phen, $BaTiO_3$-*g*-PSt-Tb^{3+} and Tb^{3+}-Phen. Four emission peaks for the three complexes appeared at almost the same position at ca. 490 nm ($^5D_4 \rightarrow {}^7F_6$), 546.5 nm ($^5D_4 \rightarrow {}^7F_5$), 584 nm ($^5D_4 \rightarrow {}^7F_4$), and 623 nm ($^5D_4 \rightarrow {}^7F_3$). From the graph it can be seen that the emission peak at 546.5 nm ($^5D_4 \rightarrow {}^7F_5$) has the strongest intensity. Moreover, the fluorescence intensity of $BaTiO_3$-*g*-PSt-Tb^{3+}-Phen is much higher than $BaTiO_3$-*g*-PSt-Tb^{3+} and Tb^{3+}-Phen. The emission peak of $BaTiO_3$-*g*-PSt-Tb^{3+}-Phen at 546.5 nm is about 29 times as higher as that of $BaTiO_3$-*g*-PSt-Tb^{3+}. The result might be due to that the introduction of the small-molecular ligand Phen, which are able to match the coordination number of Tb^{3+} ions and thus improve fluorescence intensity. Furthermore, the emission intensity of $BaTiO_3$-*g*-PSt-Tb^{3+}-Phen at

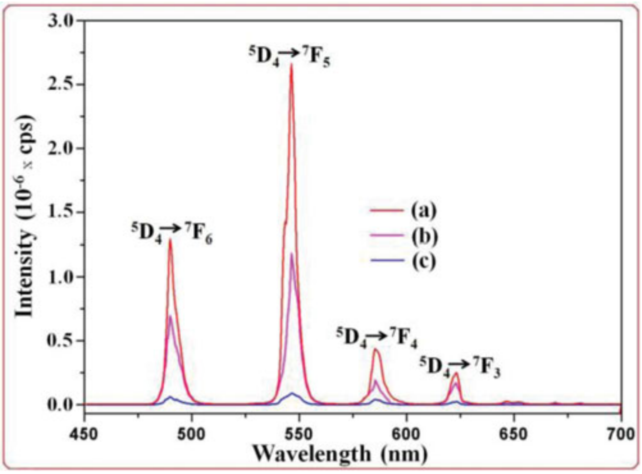

Figure 5. . Emission spectra of (a) $BaTiO_3$-*g*-PSt-Tb^{3+}-Phen, (b) Tb^{3+}-Phen, and (c) $BaTiO_3$-*g*-PSt-Tb^{3+} hybrids ($\lambda_{ex} = 328$ nm).

546.5 nm is 2.2 times higher than that of Tb^{3+}-Phen. The above comparisons reveal that the presence of $BaTiO_3$-*g*-PSt-COOH in $BaTiO_3$-*g*-PSt-Tb^{3+}-Phen has played an important role which serves not only as a macromolecular ligand coordinating with Tb^{3+} ions but also as an immobilization phase leading to a stable rigid structure and enhancing the fluorescence emission intensity. In other words, $BaTiO_3$-*g*-PSt-COOH with a large number of carboxyl groups is near Tb^{3+} ions, and the lone pair electron in the oxygen atom of COO^- transfers to the empty electron orbit of the external layer of Tb^{3+} ions to form a conjugated chelate ring.

Photographs of $BaTiO_3$-*g*-PSt-Tb^{3+}-Phen were taken at different conditions, as shown in Fig. 6. The $BaTiO_3$-*g*-PSt-Tb^{3+}-Phen is a white powder without visible fluorescence

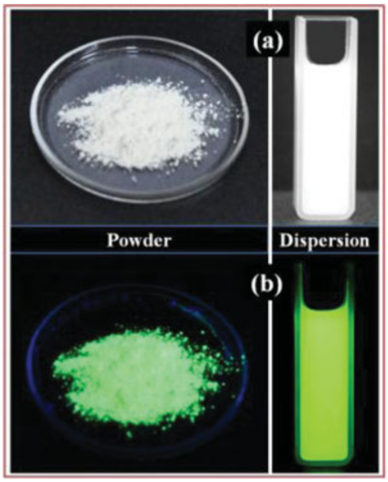

Figure 6. Photographs of $BaTiO_3$-*g*-PSt-Tb^{3+}-Phen powder and dispersion under (a) daylight and (b) 365 nm UV light.

under daylight whereas it emits a characteristic green light when subjected to UV irradiation. Although the UV light at 365 nm is not the optimum excitation wavelength, a strong fluorescence can be observed with the naked eye.

Conclusion

BaTiO$_3$-*g*-PSt-Tb^{3+}-Phen complexes were synthesized by using a combination of RAFT polymerization, substitution reaction and coordination chemistry. The FT-IR and XRD results revealed the chemical immobilization of PSt-COOH onto BaTiO$_3$. The SEM analysis corroborated the morphology of BaTiO$_3$-*g*-PSt-COOH hybrids. The TGA analysis showed the grafted PSt-COOH content of composites is 24%. The PL spectrum of BaTiO$_3$-*g*-PSt-Tb^{3+}-Phen exhibited four emission peaks, 490, 546.5, 584, and 623 nm, and the strong characteristic hypersensitive emission band of Tb^{3+} was observed at 546.5 nm due to the $^5D_4 \rightarrow {}^7F_5$ transitions.

Acknowledgment

This work was supported by the Technology Innovation Program (No. 10052923, The Development of Light Extraction Complex Substrate for Curved-OLED Lighting with High-CRI) funded by the Ministry of Trade, Industry & Energy.

References

[1] Bach, L. G. *et al.* (2013). *J. Colloid. Interf. Sci.*, *394*, 132.
[2] Panthi, G. *et al.* (2015). *J. Ind. Eng. Chem*, *21*, 26.
[3] Pontes, F. M. *et al.* (2003). *J. Lumin.*, *104*, 175.
[4] Meng, J. *et al.* (1995). *Phys. Lett. A 205*, 72.
[5] Zhang, M. S. *et al.* (2001). *Solid. State. Commun.*, *119*, 659.
[6] Verma, K. C. *et al.* (2013). *J. Alloy. Compd.*, *578*, 5.
[7] Kumari, A. *et al.* (2015). *J. Ind. Eng. Chem*, *21*, 696.
[8] Islam, Md. R. *et al.* (2013). *Appl. Surf. Sci.*, *276*, 298.
[9] Xu, Q. *et al.* (2013). *J. Colloid. Interf. Sci.*, *394*, 630.
[10] Zhao, Y., & Perrier, S. (2007). *Macromolecules*, *40*, 9116.
[11] Xie, L. *et al.* (2010). *J. Mater. Chem.*, *21*, 5897.